Semiconductor surface diffusion: Nonthermal effects of photon illumination

R. Ditchfield, D. Llera-Rodríguez, and E. G. Seebauer*
Department of Chemical Engineering, University of Illinois, Urbana, Illinois 61801

(Received 30 August 1999)

Nonthermal influences of photon illumination on surface diffusion at high temperatures have been measured experimentally. Activation energies and pre-exponential factors for diffusion of germanium, indium, and antimony on silicon change by up to 0.3 eV and two orders of magnitude, respectively, in response to illumination by photons having energies greater than the substrate band gap. The parameters decrease for *n*-type material and increase for *p*-type material. Aided by results from photoreflectance spectroscopy, we suggest that motion of the surface quasi-Fermi-level for minority carriers accounts for much of the effect by changing the charge states of surface vacancies. An additional adatom-vacancy complexation mechanism appears to operate on *p*-type substrates. The results have significant implications for aspects of microelectronics fabrication by rapid thermal processing that are governed by surface mobility.

INTRODUCTION

Diffusion on surfaces governs several process steps in microelectronics fabrication, including the formation of hemispherical grained silicon (HSG) for use in memory devices[1] as well as the filling of vias with metals for device interconnection purposes.[2] However, concomitant diffusion within bulk induces unwanted interface degradation and dopant migration in heterostructures. As a means to avoid these undesired processes, current methodology in microelectronics fabrication attempts to use low processing temperatures whenever possible. Consequently, interest has grown in nonthermal methods of modifying surface diffusivities. Photon illumination may represent one such technique, although this idea remains speculative.

Some work on electron-stimulated disordering[3,4] has indirectly hinted that photon illumination can enhance mobility.[4] However, the idea was left in embryonic form. This laboratory has independently postulated effects mediated by an interaction between charged vacancies or adatoms and illumination-induced variations in the surface Fermi energy.[5,6] However, until very recently no direct experimental evidence has materialized to back these ideas.

We have recently employed second harmonic microscopy (SHM) to obtain evidence in the cases of Ge and In on Si(111).[7] The present paper expands on that work in several ways. We extend SHM measurements down to lower temperatures where new phenomenology becomes apparent. We employ an additional adsorbate, Sb, to yield a more complete a symmetric sequence of group-III, -IV, and -V elements on a group-IV substrate. Finally, we describe photoreflectance (PR) measurements that give more insights into the electronic phenomena underlying the diffusion effects.

EXPERIMENT

Surface diffusion was measured in ultrahigh vacuum via second harmonic microscopy, an optical method we have detailed previously.[5,6,8] This method images directly the temporal evolution of a one-dimensional step concentration profile, which in turn is created with a molecular beam and retractable mask. Illumination of the profile with a pulsed Nd:YAG (yttrium aluminum garnet) laser at 1064 nm produces a small yield of surface second harmonic generation in reflection that varies with adsorbate concentration and therefore with position on the surface. Figure 1 shows a typical set of unprocessed profiles. Independent calibrations of yield vs concentration via Auger electron spectroscopy[6,8] permit direct conversion of raw second harmonic profiles into concentration profiles. Subsequent imaging processing,[6,8] followed by a straightforward Boltzmann-Matano analysis,[5] then yields the dependence of the surface diffusion coefficient D on coverage θ without parametrization. Control experiments in the present work showed that imaging itself did not perturb the profiles. Illumination during diffusion originated from either a 10-mW continuous-wave (cw) He-Ne laser operating at 632.8 nm or a 75-W Xe arc lamp. Various filters and focusing optics were combined to vary the intensity while maintaining good spatial uniformity over the diffusing profile.

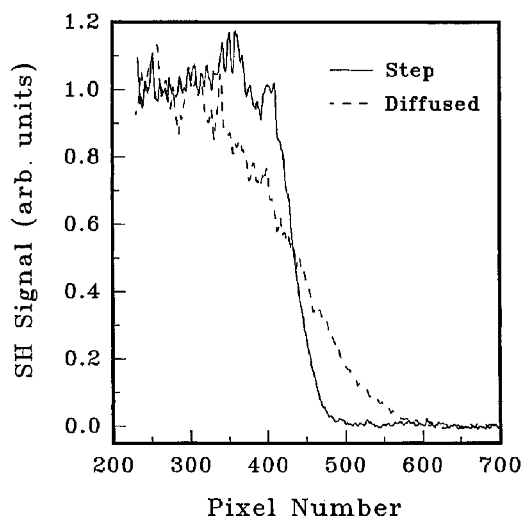

FIG. 1. Typical unprocessed second harmonic images of an initial step and diffused profile for In on Si(111). In this case diffusion took place for 90 min at 780 K under cw He-Ne illumination at 1.9 W/cm^2.

 ©2000 The American Physical Society

To help interpret the diffusion results, we monitored the position of the Fermi energy E_f at the surface by conducting a separate set of experiments with PR. PR measures the change in surface reflectance induced by a perturbing light source. The photogenerated carriers within the semiconductor change the built-in surface electric field either by neutralizing some of the built-in surface charge[9] or by decreasing the width of the surface space charge region.[10] The changes in surface electric field in turn perturb the surface reflectance R in narrow regions of wavelength corresponding to optical transitions of the substrate material.[11] The normalized reflectance change $\Delta R/R$ exhibits a spectral dependence that is monitored with a separate probe beam that is much weaker than the perturbing light. Quantitative analysis of the spectrum can yield the surface potential V_s and therefore the position of E_f at the surface. Although the theory of PR has developed enough in the last decade to make such determinations a real possibility,[12–16] significant uncertainties still exist in actual practice[14] because many factors affect the parameters derived from a PR spectrum. Nevertheless, the particular conclusions we draw from our PR results are fortunately not significantly weakened by these uncertainties.

We conducted PR in the same chamber as for surface diffusion. The optical components and setup closely resembled those of work we have previously published,[17] with the variable-wavelength probe beam at a 45° angle of incidence. The perturbing light impinged at normal incidence from the He-Ne laser referred to above, but with a mechanical chopper (400 Hz) placed in the beam for phase-sensitive detection of the induced reflectance change. We examined the wavelength range between 340–390 nm in the vicinity of the nearly degenerate[18–20] E_1 and E_0' optical transitions for Si, which lie near 3.4 eV.

Experiments were performed on Si(111) showing the standard 7×7 reconstruction in low-energy electron diffraction (LEED) and no detectable impurities in Auger spectroscopy. This work employed both n-type (As-doped, $8\times10^{17}\,\mathrm{cm}^{-3}$) and p-type (B-doped, $1\times10^{18}\,\mathrm{cm}^{-3}$) material. Molecular beams of Ge, In, and Sb originated from heated crucibles of boron nitride containing the respective elements. We found that under some conditions (especially with new crucibles), boron nitride can pyrolyze slightly to yield nitrogen contamination in the beam. Therefore, periodically we checked the surface composition after dosing with Auger spectroscopy to ensure the absence of spurious nitrogen during diffusion and photoreflectance experiments.

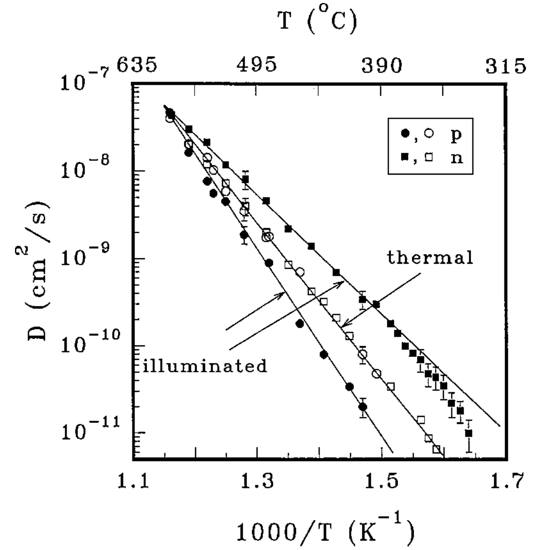

FIG. 2. Arrhenius plots for In diffusion on n- and p-type Si(111) at about 10^{18} cm^{-3} doping under dark and illuminated conditions. Illumination was with cw He-Ne light at 1.9 W/cm^2. Error bars derive from standard error analysis (Refs. 21 and 22) of the diffused profiles, while lines represent least-squares fits. For diffusion in the dark, n- and p-type material yield identical fits. For n-type illuminated material, the least-squares fit include only data above 390 K. The drop-off in D below 390 K appears to represent a true change in slope.

RESULTS

Figure 2 shows Arrhenius plots of the diffusivities D under dark and illuminated conditions for In. Measurements were limited at high temperatures by desorption of In into the gas phase, and at low temperatures by excessively long diffusion times. In all cases the data obey conventional thermally activated behavior according to

$$D = D_0 \exp(-E_{\mathrm{diff}}/kT), \tag{1}$$

where E_{diff} denotes the activation energy, D_0 the preexponential factor, T the temperature, and k Boltzmann's constant. The data fall into two temperature regimes separated at about 390 K.

TABLE I. Surface diffusion parameters on Si(111).

Adsorbate	Doping type	E_{diff} (eV) Thermal	E_{diff} (eV) Illuminated[a]	D_0 (cm^2/s) Thermal	D_0 (cm^2/s) Illuminated[a]
Sb	n	2.61 ± 0.09	2.30 ± 0.07	$6\times10^{3\pm0.6}$	$2\times10^{2\pm0.5}$
	p	2.65 ± 0.09	3.00 ± 0.08	$7\times10^{3\pm0.6}$	$4\times10^{3\pm0.6}$
Ge	n	2.44 ± 0.07	2.20 ± 0.07	$4\times10^{2\pm0.5}$	$3\times10^{1\pm0.5}$
	p	2.44 ± 0.07	2.71 ± 0.07	$4\times10^{2\pm0.5}$	$4\times10^{3\pm0.5}$
In	n	1.78 ± 0.04	1.48 ± 0.04	$1\times10^{3\pm0.4}$	$4\times10^{1\pm0.4}$
	p	1.78 ± 0.04	2.10 ± 0.04	$1\times10^{3\pm0.4}$	$4\times10^{4\pm0.4}$
In[b]	n	1.78 ± 0.04	1.81 ± 0.07	$1\times10^{3\pm0.4}$	$1\times10^{4\pm0.5}$

[a]Below 1130 K except where noted. Illumination with He-Ne laser at 1.9 W/cm^2.
[b]Below 930 K.

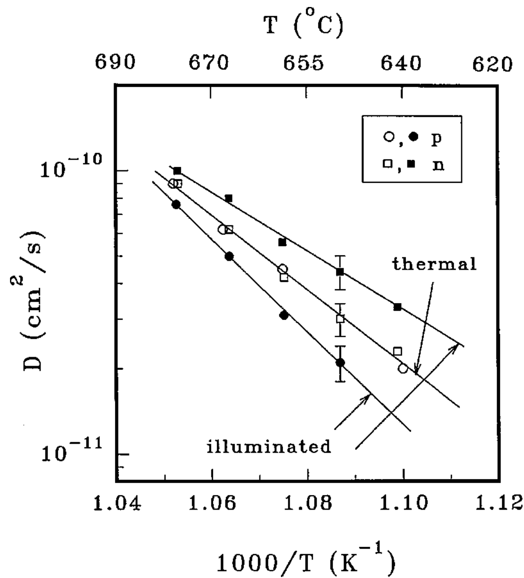

FIG. 3. Arrhenius plots for Sb diffusion on n- and p-type Si(111) at about 10^{18} cm^3 doping under dark and illuminated conditions. Illumination was with cw He-Ne light at 1.9 W/cm^2.

Most of the data above 390 K have been reported previously,[7] although we will summarize the salient features here. The results without illumination remain independent of doping type, but illumination produces a family of convergent Arrhenius plots, with D rising for n-type doping and falling for p-type doping. Table I summarizes the corresponding values of E_{diff} and D_0 at the maximum intensity we investigated of 1.9 W/cm^2. Both E_{diff} and D_0 vary logarithmically with intensity, in opposite directions with roughly equal magnitude for the two kinds of bulk doping. Parameters with broadband illumination match those for He-Ne illumination.

In the present measurements extended to lower temperatures, another phenomenon appears. Below 390 K, D for illuminated n-type material begins to drop below the line extrapolated from higher temperatures. The effect is rather modest (up to a factor of about 2), but definitely cannot be accounted for by experimental error. The Arrhenius parameters in this range increase to $E_{diff}=1.81$ eV and $D_0=1\times10^4$ cm^2/s. The activation energy thus closely matches the thermal value, while the prefactor falls an order of magnitude higher than in the thermal case.

Results for Ge have been reported previously.[7] Briefly, Ge shows a family of convergent plots below 1110 K resembling those for In above 390 K. Table I includes numerical values for E_{diff} and D_0. Interestingly, while the exact values for Ge and In differ, the photoinduced *changes* in these parameters remain identical. For Ge above 1110 K, the Arrhenius plots merge with the purely thermal data. LEED patterns near the isokinetic temperature reveal a gradual transition from 7×7 symmetry near 1060 K to 1×1 symmetry near 1110 K.

Figure 3 shows Arrhenius plots for Sb. For Sb (as well as the other adsorbates described above), diffusion was measured for coverages θ up to about 0.6 ML. Boltzmann-Matano analysis showed that in all cases D remains independent of θ in this range, in accord with thermal results for Sb, Ge, and In.[6,8] The convergent lines for Sb in Fig. 3 mimic the behavior for In and Ge. Measurements were limited at high temperature by Sb desorption. Table I shows that the photoinduced changes in Arrhenius parameters match those for the other adsorbates.

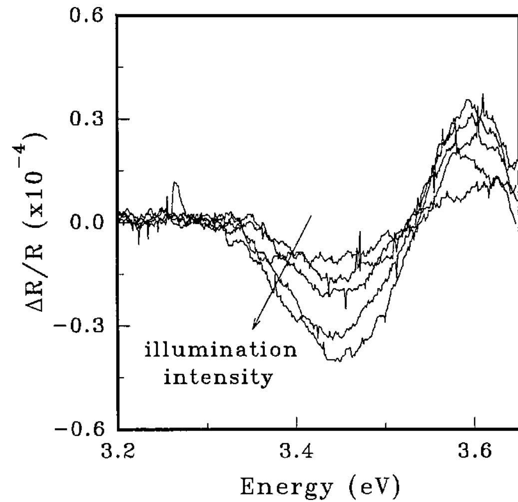

FIG. 4. Photoreflectance spectra at 300 K of the Si E_1 transition with 0.7 ML of In on n-type material. Different curves represent He-Ne illumination intensities of 0.15, 0.24, 0.46, 0.97, 1.4, and 1.9 W/cm^2.

Figures 4 and 5 show room-temperature PR spectra at various illumination intensities for n- and p-type Si, respectively. The surfaces supported 0.6 ML of In in each case. The spectra exhibit shapes characteristic of the classic third-derivative functional form expected for electromodulation spectroscopies of this at optical transitions far from the fundamental band gap. This functional form has been described in detail by Aspnes,[11] and can be written as

$$\Delta R/R=\mathrm{Re}[Ce^{i\phi}(E-E_{crit}+i\Gamma)^{-n}], \quad (2)$$

where C denotes an amplitude factor, ϕ a phase factor, Γ a phenomenological broadening parameter, and E_{crit} and n the energy and dimension of the critical point associated with the transition. Choosing the parameter n becomes tricky when employing a single line-shape equation to describe two nearly degenerate transitions. Less than 0.1 eV separates the E_1 and E_0' transitions of Si.[19] The E_1 takes place along the Λ

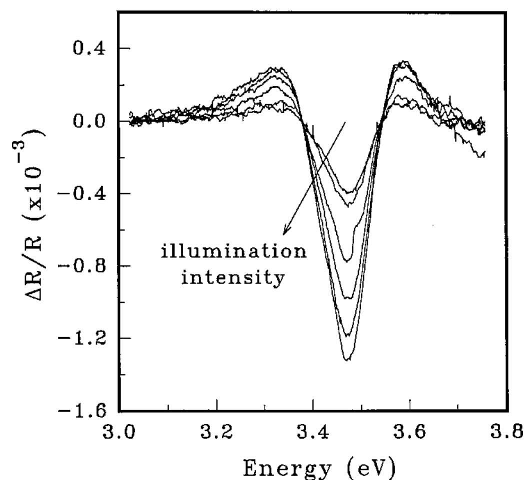

FIG. 5. Photoreflectance spectra as in Fig. 4 for p-type material.

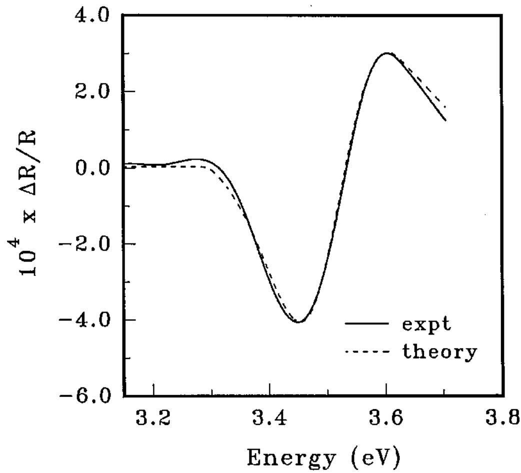

FIG. 6. Comparison of smoothed photoreflectance spectrum from Fig. 4 (n-type material) at 1.9 W/cm^2 and 300 K with theoretical low-field expression of Eq. (2). Experimental conditions did not affect ϕ and Γ, which remained at 90° and 150 meV, respectively. The remaining parameters derived from Eq. (2) for this spectrum were $E_{\rm crit}=3.457$ eV and $C=2.60\times10^{-5}$.

points within the Brillouin zone, while the E_0' lies at the Γ point. Not surprisingly, different line shapes describe the well-resolved transitions at low temperature: an excitonic form for E_1 and a two-dimensional form for E_0'.[19] Near room temperature where the optical transitions become unresolvable, one must resort to phenomenology. We chose $n=3$, corresponding to the line shape for a three-dimensional critical point,[11] as providing the best fit to the data and consistent with previous electroreflectance reports.[24] The remaining parameters in Eq. (2) could then be determined from experimental spectra using the three-point method of Aspnes and Rowe.[25] Fits of Eq. (2) to the representative spectra from n- and p-type material appear in Figs. 6 and 7, respectively. The match is satisfactory. We found that ϕ and Γ depended

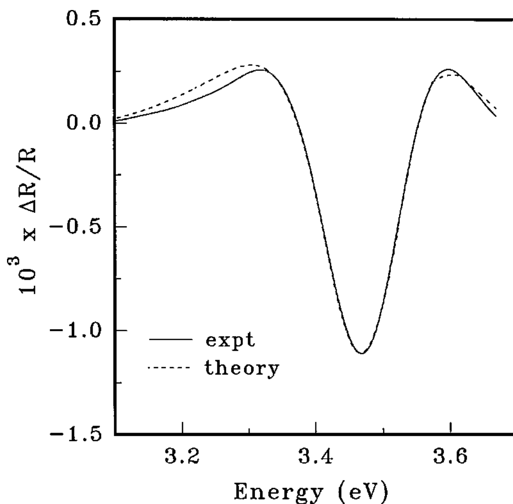

FIG. 7. Comparison of smoothed photoreflectance spectrum from Fig. 5 (p-type material) at 1.9 W/cm^2 and 300 K with theoretical low-field expression of Eq. (2). Experimental conditions did not affect ϕ and Γ, which remained at 130° and 160 meV, respectively. The remaining parameters derived from Eq. (2) for this spectrum were $E_{\rm crit}=3.546$ eV and $C=1.11\times10^{-4}$.

only on material type, remaining independent of other conditions. The amplitude C depended on material type, temperature, and illumination intensity. $E_{\rm crit}$ decreased linearly with temperature, in agreement with the Varshni relation[19] for Si in this temperature range:

$$E_{\rm crit}=E_{\rm crit,0}-\lambda T. \tag{3}$$

However, the exact values of the parameters $E_{\rm crit,0}$ and λ we found deviated slightly from those measured by ellipsometry[19] and PR,[12] which in turn differed slightly from each other. We attribute these differences to the phenomenology required to fit two transitions that merge together in the temperature range of interest with a single line shape.

A principal goal of the PR experiments was to determine whether the adsorbed species affected the position of the surface Fermi level. Experiments with clean and In-adsorbed surfaces (up to $\theta=0.7$) revealed no change in any parameter, showing without further quantitative analysis that E_f at the surface remained unchanged upon adsorption.

A second goal of the PR experiments was to estimate the precise position of E_f at the surface. Usually such estimates employ the spacing between the Franz-Keldysh oscillations that occur in PR spectra taken at the E_0 optical transition lying near the material band gap.[14] These oscillations appear when the broadening parameter Γ is sufficiently small that the more generalized Airy-function expressions for $\Delta R/R$ become appropriate.[14] With careful effort, calculating the surface electric field using Franz-Keldysh oscillations can approach an accuracy of 5%[14] so that the calculation of E_f (which varies with the maximum electric field $\mathcal{E}_{\rm max}$ as $\mathcal{E}_{\rm max}^{1/2}$) could conceivably approach the actual value within 2–3 %.

However, at other optical transitions Γ is usually large enough to broaden out these oscillations (which are indeed not observed in our spectra), and the third-derivative functional form becomes more appropriate. The amplitude factor C contains the principal information regarding surface potential, although C is also affected by numerous other effects. Unfortunately, using amplitude data alone probably leads to results that are considerably worse than using Franz-Keldysh oscillations. Probably for this reason, there appears to be only one other attempt to extract the surface potential from C,[12] and the results were not checked by an independent method. Such a check would have been very useful, because, for example, it is known that even a fairly weak probe beam induces a photovoltage (in addition to that from the perturbing laser) that decreases the apparent surface potential (by up to more than 30%) unless extraordinary measures are taken to avoid this problem.[14,15] We have not taken such precautions here. Nevertheless, we expect that our calculations are probably good to within 0.2 eV or so, which is sufficient for the limited conclusions we wish to draw.

Figures 8 and 9 show C plotted as a function of illumination intensity for n- and p-type material at several temperatures. For both kinds of material, spectral amplitude decreases rapidly with T, yielding unusably small signals by 400 K. This phenomenon is well known in PR of semiconductors,[12,26] but unfortunately it limited our PR work to temperatures significantly below those of the diffusion experiments.

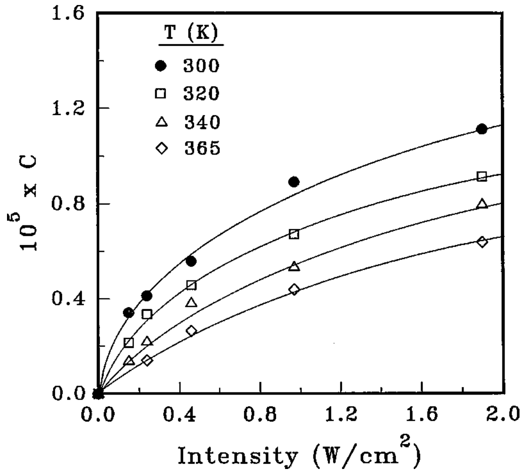

FIG. 8. Variation of the photoreflectance amplitude factor C with illumination intensity for the spectra in Fig. 6 (n-type material). Lines represent logarithmic fits according to Eq. (7).

For the doping levels and illumination intensities used in this work, illumination does not perturb the majority carrier density sufficiently to change $\mathcal{E}$ at the surface by collapsing the width of this region. Instead, illumination affects $\mathcal{E}$ by neutralizing surface charge and thereby generating a photovoltage that changes the surface potential V_s. In such cases, methods have been recently developed[24,35] for using C to calculate V_s in the absence of illumination as well as the change in surface potential ΔV_s induced by illumination.

The method works as follows. The PR amplitude factor C scales linearly in ΔV_s.[27,26] In turn, ΔV_s obeys the following relation:[13,14]

$$\Delta V_s = \frac{\eta k T}{q} \ln\left[\frac{J_{pc}}{\rho J_0} + 1\right]. \tag{4}$$

Here, J_{pc} denotes the photoinduced current density to the surface, J_0 the corresponding dark current density, q the electronic charge, ρ an area factor, and η a quantum-mechanical ideality factor. While η usually lies near unity,[14,15] ρ can be quite small due to the differing areas where dark current is nominally discharged (on surface

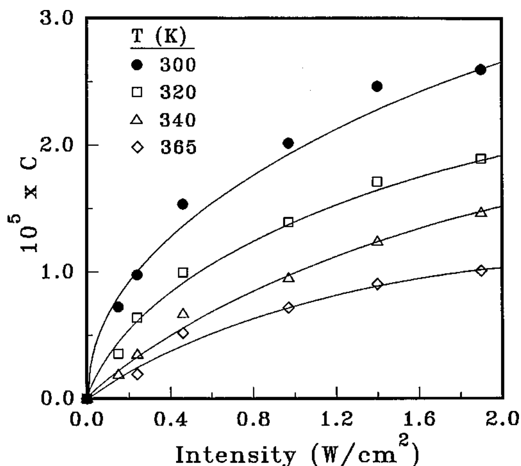

FIG. 9. Variation of the photoreflectance amplitude factor C with illumination intensity for the spectra in Fig. 7 (p-type material). Lines represent logarithmic fits according to Eq. (7).

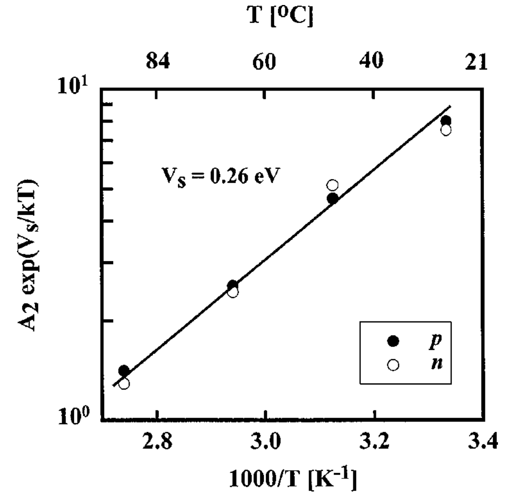

FIG. 10. Arrhenius plots of the quantity $A_2 \exp(V_s/kT)$ of Eq. (7) taken from the data of Figs. 8 and 9. The slopes give $V_s = 0.26 \pm 0.02$ eV for both n- and p-type material. As discussed in the text, this value probably underestimates V_s.

states, which may be a small fraction of the surface atom density) vs photocurrent (the entire illuminated area).[14,15] The photocurrent J_{pc} scales linearly in intensity I according to[14,15,27]

$$J_{pc} = \frac{q I \gamma (I - R)}{h \nu}\left[1 - e^{-\alpha W} + \frac{\alpha L_d}{1 + \alpha L_d} e^{-\alpha W}\right], \tag{5}$$

where R represents the reflectivity (0.4 for Si at 632.8 nm), γ the quantum efficiency [0.6 for Si (Ref. 24)], h Planck's constant, v the frequency of the light, α the absorption coefficient, W the depletion width, and L_d the diffusion length of the minority carriers. The dark current J_0 to the surface represents thermal carrier generation and contains V_s according to[14,28]

$$J_0 = A^{**} T^2 \exp(-V_s/kT), \tag{6}$$

where A^{**} denotes the modified Richardson constant of 3.2×10^5 A/m^2 K^2 for p-type Si(111) and 11.2×10^5 A/m^2 K^2 for n-type Si(111).[29,30] Equations (4)–(6) together with the linearity of C with ΔV_s imply a relation between C and V_s of the form

$$C = A_1 \ln\{A_2 I \exp(V_s/kT) + 1\}, \tag{7}$$

where A_1 and A_2 represent constants containing the various parameters in Eqs. (4)–(6) together with parameters describing the optical properties of the substrate.[31] Fitting Eq. (7) to a set of data for C collected at varying intensities yields the combined parameter $A_2 \exp(V_s/kT)$. Experiments at different temperatures yield an Arrhenius plot of this combined parameter, giving an average value for V_s over the temperature range of measurement.[32]

Figure 10 shows an Arrhenius plot of $A_2 \exp(V_s/kT)$ obtained by this procedure. The extracted value of V_s lies at 0.26 ± 0.02 eV for both n- and p-type material. The result agrees fairly well with the 0.3-eV surface potential obtained by Fujimoto *et al.*[12] by a very similar method. Since illumination in PR acts to flatten the bands and since E_f in the bulk already lies close to the conduction and valence bands, the

magnitude of our data is consistent with pinning of the surface Fermi level deeper within the band gap. As we have said, our values for V_s probably underestimate the true values significantly. Thus, we consider our data to be consistent with near-midgap pinning, in agreement with other work as discussed below.

DISCUSSION

The importance of ionization effects

Certain features of our results yield to straightforward interpretation. The influence of doping type and the importance of the condition $h\nu > E_g$ point to a driving mechanism that is electronic rather than vibrational. Quantitative analysis requires examination of what our experiment really measures: the mass transfer diffusivity D_M. This quantity comprises the product of the more well-known intrinsic diffusivity D_I and the fractional coverage θ of mobile adatoms:[33,34]

$$D_M = \theta D_I . \tag{8}$$

The distinction between D_M and D_I is important because in our experiments, θ falls far below the nominal adsorbate coverage. On Si(111), adsorbates from groups III, IV, and V of the Periodic Table substitute for surface Si atoms so that most adsorbate is rendered essentially immobile.[5,8,33,35] Molecular-dynamics simulations have shown[8,36] that diffusional motion takes place via the formation of adatom-vacancy pairs, in close analogy to vacancy diffusion in the bulk. In a conventional thermodynamic framework, the measured values for E_{diff} and D_0 therefore contain contributions from the enthalpies and entropies of adatom-vacancy pair formation as well as those of intrinsic adatom motion. Thus, photon illumination can in principle affect either or both of the intrinsic and adatom-vacancy contributions.

Our data show that illumination increases E_{diff} by up to 0.3 eV on *p*-type Si and decreases E_{diff} by the same amount on *n*-type Si, for a total swing of 0.6 eV. For Ge on Si, the entire intrinsic migration energy is only about 0.6 eV (Ref. 8) suggesting that most of the observed effects originate from vacancies. Furthermore, the insensitivity of the photon-induced changes to adsorbate type points to an underlying commonality, presumably vacancies on the Si surface.

The vacancy contribution to mass transfer diffusion through θ implicitly includes the charge state of the vacancy. In the bulk, Si vacancies take on charge states ranging from $+1$ to -2.[37] Effects of vacancy ionization on bulk diffusion are well documented, with D_M obeying[37]

$$D_M = ([V^+] + [V^x] + [V^{2-}]) D_{0,I} \exp(-E_{\mathrm{diff},I}/kT), \tag{9}$$

where the subscript *I* refers to intrinsic diffusion. Each vacancy concentration $[V^j]$ varies as $\exp(-\Delta G_I^j/kT)$, where ΔG_I denotes the free energy of ionization. Since charge transfer between the Fermi energy E_f and a vacancy level is required for ionization, the relative populations of differing charge states depends on the energy difference between E_f and these levels, and therefore on doping type and concentration. To our knowledge, the charge states available to a vacancy on Si(111)-(7×7) remain unknown. Defect structures on Si(111)-(7×7) have been investigated only recently, but calculations for intrinsic Si indicate that each dangling bond of a vacancy supports roughly two-thirds of the charge density of the corresponding filled-site dangling bond.[38] Presumably this number varies with the availability of charge carriers. Furthermore, significant experimental evidence exists that charged vacancies can exist on group-IV semiconductors,[6] so that an equation analogous to Eq. (9) governs surface diffusion as well.

Further evidence for the importance of ionization comes from the similarity in temperatures for convergence of the Arrhenius plots and for disappearance of the 7×7 surface reconstruction in the Ge/Si system. Thermal diffusion parameters remain invariant as the surface transforms from 7×7 to 1×1 at high temperature, suggesting that long-range order by itself plays no important role. The insensitivity of In and Sb diffusion to surface concentration[6] confirms this notion, as both In (Ref. 39) and Sb (Ref. 40) pass through several reconstructions as the concentration and/or temperature increase with no visible effect on *D*. Thus, the photon-induced effects seem to require some other governing process.

Equation (9) predicts that purely thermal diffusion should not vary with doping type if we assume that the surface Fermi level E_f remains pinned at the same location near midgap for both *n*- and *p*-type material. Our own data for V_s are not inconsistent with this notion, given the potentially significant systematic errors we have discussed. In the literature, near-midgap pinning for Si(111)-(7×7) has indeed been reported for undoped material at room temperature.[41] For the 2×1 reconstruction, pinning position remains independent of substrate doping,[42] making this independence plausible for 7×7. No studies of high-temperature pinning exist to our knowledge for Si(111), but for Si(100)-(2×1) the pinning level remains constant to within 0.1 eV up to 1200 K.[43] Hence, under dark conditions the electronic occupation of energy levels should remain independent of bulk doping type. Equation (9) then predicts an invariance of thermal diffusivities with doping, in accord with our observations.

Failure of the conventional picture

Clearly, the simple thermodynamic framework underlying Eq. (9) provides a useful perspective for explaining many of our results. However, Eq. (9) falls short in an important respect: the decrease of D_M for *p*-type material. In general, the population of uncharged vacancies remains invariant with changes in Fermi-level position.[37] Thus, if illumination forms charged vacancies, Eq. (9) indicates that these extra species must increase D_M. However, for *p*-type material below 1100 K, D_M decreases in response to illumination.

One could argue that vacancies on the dark surface are mostly charged, and that illumination of *p*-type material simply reduces the number of charged vacancies so that D_M decreases. Several lines of evidence argue against this possibility, however. *Ab initio* calculations show that the 7×7 reconstruction of clean Si supports much larger separations of charge than does the 1×1, up to the equivalent of one full electron.[44] Presumably ΔG_I would differ for the two reconstructions, leading to differences in E_{diff} and D_0. Yet the diffusion data for the dark surface show no change in *D* throughout the transition between reconstructions at 1110 K.

Furthermore, molecular-dynamics simulations of Ge surface diffusion on Si(111)-(1×1) extrapolate nearly perfectly over experimental data on the 7×7 surface.[8] These simulations incorporate no effects of ionic charge. While the correspondence may be coincidental, it suggests that the vacancies (and adatoms) responsible for thermal diffusion on the 7×7 remain uncharged. Finally, D increases for illuminated n-type material. This fact requires that the total vacancy concentration increase in this case, implying an even greater degree of vacancy charging than for the dark surface. There exists no evidence that surface vacancies can support so much charge.

The data for n-type material present other problems for Eq. (7) as well. In particular, D_0 decreases significantly. Decomposition of ΔG_I into an enthalpy and entropy of ionization according to

$$\Delta G_I = \Delta H_I - T\Delta S_I \tag{10}$$

leads to the relation

$$D_0 = D_{0,I}\exp(\Delta S_I/k). \tag{11}$$

A nonzero ionization entropy results from the softening of phonon modes in the vicinity of the vacancy if the charge remains localized.[45] This effect results in a positive value for ΔS_I, regardless of the sign of the charge on the vacancy. Thus, D_0 cannot decrease as vacancies become more charged, counter to the experimental observation.

Some possible resolutions

We seek to explain both the general magnitude of changes in the Arrhenius parameters and the decrease in D_M for p-type material. Diagrams of the energy bands near the surface at diffusion temperatures will aid both discussions. Such diagrams appear in Fig. 11. In addition to the assumption of near-midgap pinning as suggested by our PR results, these diagrams also make the assumption that electronic occupancy within the conduction and valence bands near the surface obeys a description incorporating quasi-Fermi-levels within the so-called thermionic limit.[28,46,47] Photogenerated electrons and holes in semiconductors thermalize rapidly within the conduction and valence bands, respectively. This quasithermalization splits the Fermi level into two quasi-Fermi-levels[48] F_n and F_p that, respectively, define the electron and hole concentrations within these bands. The thermionic limit requires that F_n and F_p remain far from the band edges, which our calculations confirm. Furthermore, the thermionic limit requires that the drift velocity v_d of carriers in the surface space-charge region greatly exceed the surface recombination velocity v_r so that the quasi-Fermi-levels remain flat up throughout the space-charge region up to the surface.[28,46,47] The condition $v_d \gg v_r$ is equivalent to[28]

$$\mu\mathcal{E}_{\max} \gg v_{\text{mean}}/4, \tag{12}$$

where μ denotes the mobility and v_{mean} the mean thermal velocity of the charge carriers (equal to $(8\,\text{kT}/\pi m^*)^{1/2}$, with m^* the effective mass). For Si with a carrier concentration of $10^{18}\ \text{cm}^{-3}$ we calculate $\mathcal{E}_{\max} \sim 300\ \text{kV/cm}$, giving $v_d \sim 1000 v_r$ and justifying the use of the thermionic limit.

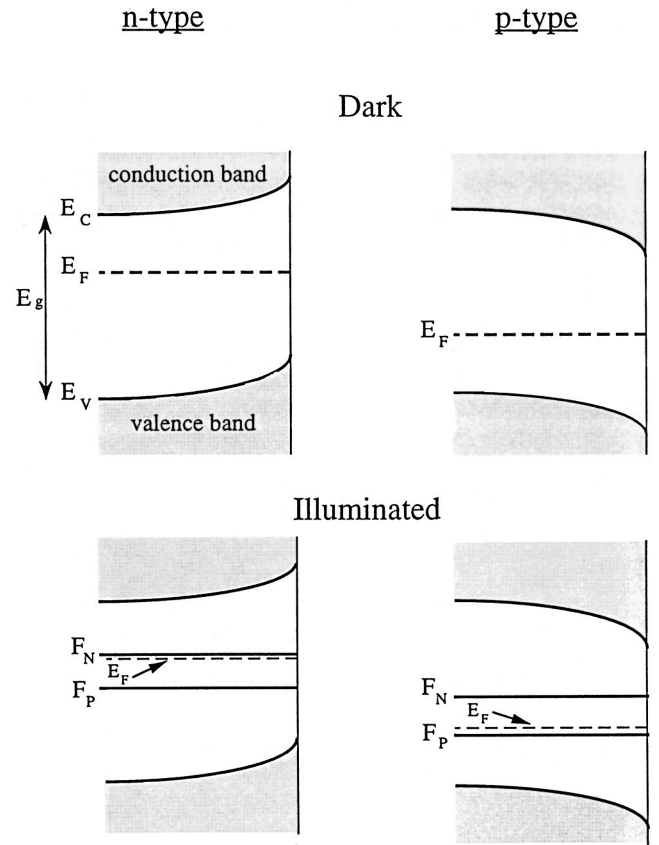

FIG. 11. Proposed near-surface band diagrams for dark and illuminated conditions on n- and p-type Si, shown schematically. In the dark, pinning of the surface Fermi energy E_f near midgap induces the conduction-band minimum E_C and valence-band maximum E_v to bend near the surface. E_f itself remains constant throughout the semiconductor. Under illumination in the thermionic limit, quasi-Fermi-levels F_n and F_p for electrons and holes split from E_f, but remain constant with respect to vacuum throughout the semiconductor. Positions of E_f, F_n, and F_p are drawn to estimation according to calculations employing standard theory for photon absorption (Refs. 23 and 24) under the conditions of our experiment. Illumination of itself does not change the band bending; photovoltage largely disappears in Si by 400 K.

Figure 11 also shows that the band bending does not change upon illumination. This assumption is equivalent to assuming zero photovoltage ΔV_s. Clearly bands do flatten near room temperature under the conditions of photoreflectance; indeed, at high-carrier concentrations a nonzero photovoltage is required to see any PR signal whatsoever. However, our own PR measurements and others[12] show that photovoltage in Si largely disappears above about 400 K. This disappearance results from the very strong temperature dependence of the dark current J_0 in Eq. (6), which also appears in the expression of Eq. (4) for ΔV_s. Above about 400 K, the dark current swamps the photocurrent and makes it ineffective in affecting V_s, so that photoinduced band bending is not an issue in our diffusion measurements.

Figure 11 shows schematically how the quasi-Fermi-levels F_n and F_p split asymmetrically, with the level corresponding to the minority carrier moving more. The precise amounts of motion are approximate, and were calculated in the following way. Light at 632.8 nm from the He-Ne laser is

absorbed over a characteristic depth of about 2 μm, which is considerably deeper than the 0.2 μm depth of the space charge region in our substrates. To a first approximation, the excess carrier concentration for the bulk can then be estimated by assuming uniform absorption in a layer of thickness 2 μm and using the known incident photon flux, the surface reflectivity, and an estimate for the excess carrier lifetime τ. In the presence of large photon fluxes, a nearby (defected) surface, and an unknown concentration of traps and defects in the bulk, making the estimate for τ no easy task. We assumed a typical value of 2 μs,[49] which could easily be off by an order of magnitude but will suffice for the present purpose. The excess electron and hole concentrations δn and δp can then be used to calculate F_n and F_p according to

$$n+\delta n=N_c \exp[-(E_c-F_n)/kT], \tag{13a}$$

$$p+\delta p=N_v \exp[-(F_p-E_v)/kT], \tag{13b}$$

where N_c and N_v represent the effective densities of states in the conduction and valence bands, and n and p the surface carrier concentrations in the dark. Finally, with the benefit of the thermionic limit the quasi-Fermi-levels are simply extended all the way to the surface.

Figure 11 shows that in the dark, midgap pinning of E_f renders the surface essentially intrinsic with respect to carrier concentration: $n\approx p$. However, illumination moves the quasi-Fermi-level for the bulk minority carriers far more than for the majority carriers, thus rendering the surface of n-type material essentially p type and *vice versa*. Thus, the surface vacancies tend to become more positively charged on n-type material and more negatively charged on p-type material. More quantitatively, the magnitude of the motion in our crude calculation is of order 0.3 eV for both n-and p-type material: identical to the magnitude of the shifts in E_{diff}. This correspondence, together with the logarithmic dependence of F_n (or F_p) and E_{diff} in illumination intensity I, all suggest a close correspondence between mass transfer diffusion and the minority-carrier quasi-Fermi-level via vacancy ionization.

It may seem significant at first that the intensity dependence of E_{diff} and ΔV_s (proportional to the PR parameter C) both vary logarithmically with I and change in opposite directions for n- and p-type material. Indeed, illumination increases both photocurrent and minority-carrier density in ways that propagate logarithmically into E_{diff} and ΔV_s with opposite sense for n- and p-type semiconductors. However, much of the correspondence between E_{diff} and ΔV_s is almost certainly coincidental. These quantities were measured at very different temperatures. More importantly, the balance between photocurrent and dark current (both involving mainly *majority* carriers) drives changes in ΔV_s while changes in the *minority*-carrier quasi-Fermi-level drives changes in E_{diff}. Thus, while ΔV_s changes a great deal at room temperature, it moves hardly at all at diffusion temperatures. The effects of T on F_n and F_p are not nearly so large.

So exactly how much should the minority-carrier quasi-Fermi-level affect E_{diff}? We cannot say for certain because the answer depends upon how minority carriers thermalize themselves with vacancy levels lying deep within the band gap. The details of carrier recombination with deep levels at surfaces remain incompletely understood at present. However, it is well known that deep-lying surface states on semiconductors can take considerable time (milliseconds[14] to hours[50]) to thermalize with the bulk under illumination. However, vacancies have a lifetime τ_v of only microseconds under the conditions of our experiment.

This estimate comes from the following calculation for Ge on Si. Previous molecular-dynamics calculations in this group for the intrinsic diffusivity D_I yield an activation energy of 0.59 eV and a prefactor of 2×10^{-3} cm^2/s.[8] Using these numbers together with the relations $\theta=D_M/D_I$ and $\theta=\exp(-\Delta G_f/kT)$, with $-\Delta G_f$ denoting the free energy of vacancy formation, we find that θ is of the order 10^{-4} under the conditions of our experiment. The recombination rate R_{va} of vacancies with adatoms can be estimated assuming a simple diffusion-limited reaction expression:

$$R_{va}=k_r[V][\mathrm{adatoms}]. \tag{14}$$

The reaction constant k_r is given to a first approximation by[51]

$$k_r=2\pi D_I \ln \sqrt{1/\theta}. \tag{15}$$

Since to a good approximation [adatoms]$\approx[V]$, insertion of easily-calculated values for D_I and $[V]=N_s\theta$ (where N_s denotes the surface atom density of the substrate) yields a good estimate for R_{va} and therefore the vacancy lifetime through $\tau_v=[V]/R_{va}$. Thus, if the energy states of the vacancies communicate poorly with the carriers in the bulk, it is quite possible that the vacancy charge distribution never reaches what a simple equilibrium calculation might predict.

Other nonthermal effects may also play a role. Enhanced diffusion of defects in bulk GaAs due to local energy dissipation by nonradiative electron-hole recombination has been observed[52] and modeled.[53] That particular work concerned excess carrier injection in a diodelike structure, but photogeneration should be equally capable of producing the observed effects. Unfortunately, diffusional enhancement is expected by this mechanism, while the present experiments reveal both enhancement and inhibition. Other phenomena arising from the substantial drift velocity of minority carriers impacting the surface may be important, but we are unaware of an adequate theory to invoke a more detailed description.

With respect to the decrease in D_M for p-type substrates, we speculate that adatoms form complexes with surface vacancies under illumination. Such complexes are well known to form within the bulk, where the interaction can be mediated by electrostatic[54,55] or lattice strain[56,57] forces. However, such complexes should behave differently on a surface than in the bulk. In bulk vacancy diffusion, the constraints of a three-dimensional lattice require that when an atom moves, the corresponding vacancy moves in the opposite direction at the same rate. In other words, the motion of vacancies and foreign atoms are completely coupled. This coupling does not necessarily hold on a surface. Once an adatom-vacancy pair forms, the adatom may wander freely independent of the vacancy. Indeed, molecular-dynamics simulations show that adatoms generally move much faster than surface

vacancies.[36] Thus, interactions that couple adatoms to vacancies may slow the rate of intrinsic adatom hopping and thereby decrease D_M.

A coupling mechanism may be easily envisioned on *p*-type Si. As Fig. 11 indicates, illumination renders the surface of *p*-type Si more *n*-type, and presumably increases the average negative charge on the vacancies. The charges on adatoms like Ge, In, and Sb are currently unknown. However, *ab initio* calculations for the Si(111)-(7×7) surface suggest that Si atoms in so-called ''adatom'' positions in the structure (i.e., in the most exposed positions and presumably most likely to diffuse) carry some positive charge. If this finding generalizes to the adsorbates examined here, then presumably an electrostatic attraction could exist between the negative vacancies and positive adatoms.

If adatoms remain positively charged on *n*-type material, coupling would vanish with the now-positive vacancies. Thus, D_M could increase with illumination according to Eq. (7) because both neutral and positively charged vacancies would contribute. Note that this picture only explains why D_M decreases for *p*-type material and increases for *n*-type material. It does not explain the Arrhenius parameters themselves. Specific arguments concerning E_{diff} remain difficult to make because they depend heavily on the ionization enthalpy ΔH_I. This quantity depends upon the positions of the energy states of the various charged vacancies, which remain unknown. D_0 for *p*-type material admits a straightforward explanation: participation of ionized vacancies introduces a positive ionization entropy ΔS_I into the prefactor as discussed above, making D_0 increase. However, the decrease in D_0 for *n*-type material admits no easy explanation. In the bulk, ΔS_I is always positive regardless of the sign of the vacancy charge. We can only speculate that a qualitative difference in phonon mode softening sometimes exists when comparing the bulk and the surface. While in its normal state the Si bulk contains no charge separation, such separation inheres in the very nature of Si(111)-(7×7). It may be that positively charged vacancies can actually harden the vibrational structure of this complex surface.

We also cannot easily explain the change in Arrhenius parameters below about 370 °C for In on *n*-type Si. Similar effects do not appear for Ge and Sb, although measurements for those adsorbates took place at appreciably higher temperature—above 640 °C. We speculate that exchange of In adatoms with kinks or step vacancies instead of terrace vacancies may become important at sufficiently low temperatures. Indeed, this change in mechanism explains why Arrhenius parameters for conventional surface diffusion on both metals and semiconductors often decrease dramatically when T falls appreciably below 50% of the substrate melting temperature T_M.[11] In the present case, 370 °C corresponds to $T/T_M = 0.38$—well within the range where such a transition can be expected. Granted, the diffusion parameters for In without illumination exhibit no observable changes, and the parameters with illumination increase rather than decrease. However, we understand too little about the effects of illumination on adatom production from terraces to generalize the picture to steps or kinks. Furthermore, the observed increases in E_{diff} and D_0 may have little direct physical significance if the transition between regimes is gradual.

Significance for microelectronics fabrication

Rapid thermal processing (RTP) is finding ever-increasing application in the fabrication of microelectronic devices. RTP employs lamps for wafer heating that operate at intensities at least as high as those reported here. The present results have significance for RTP processes that involve semiconductor surface diffusion. For example, surface diffusion plays a major role in the formation of epitaxial silicon by chemical vapor deposition. At sufficiently low temperatures, decreased mobility of the depositing atoms results in unwanted defects. The present results suggest that the ultimate minimum processing temperature in RTP may differ for *n*- and *p*-doped material. No such difference should exist in conventional furnace processing. In another example, surface diffusion governs the formation of hemispherical grained silicon (HSG), which is used to form electrodes for the capacitors in memory devices. HSG is formed by heating highly doped amorphous silicon in an RTP configuration to the point of incipient crystallization. Crystallites form at the free interface and grow via surface diffusion, mushrooming out of the surface as they do so.[58] The resulting roughening greatly increases the surface available for charge storage and therefore the capacitance of the device. Too much crystallization smoothens the surface and ruins the device; the precise temperature dependence of surface diffusion is therefore crucial to know. The present results predict that surface diffusivities of Si over the growing crystallites should deviate from thermal values.

We have shown that illumination affects surface diffusion on semiconductors through charged vacancies. No doubt similar phenomena can also occur in the bulk when diffusion proceeds by a vacancy mechanism. For some time it has been known that doping type and level affects bulk diffusion by altering Fermi level and therefore the concentrations of vacancies having different charge states.[18,54] Presumably the populations of such states near a free surface or near a shallow-lying discontinuity in doping concentration could also be affected by strong illumination.

From a technological perspective, such situations occur increasingly often in integrated circuit manufacture during the formation and annealing of shallow junctions by RTP. New generations of *pn* junctions are slated to lie less than 20 nm from the surface[59]—easily within the penetration depth of the incident light. Thus, motion of dopants during RTP could take place with rates significantly different from predictions based on reported thermal diffusivities. Furthermore, the diffusion rates would increase for one type of doping and decrease for the other. This asymmetry could create problems for conventional complementary metal-oxide semiconductor technologies, in which both kinds of doping are present on a single wafer.

CONCLUSION

This paper has provided strong evidence that illumination-induced movements in surface quasi-Fermi-levels can affect high-temperature surface diffusion, mainly by changing the formation energy for adatom-vacancy pairs. We expect that such phenomena can generalize to bulk diffusion, with significant implications for RTP processing. However, significant questions remain about the precise

mechanisms that govern the surface effects. For example, while the position of the quasi-Fermi-level for minority carriers appears to control the change in diffusional activation energy, the magnitude of the change depends upon just how efficiently minority carriers thermalize themselves with deep-lying vacancy levels. Also, the proposed complexation mechanism between adatoms and vacancies to yield a decrease in diffusivity for *p*-type material remains speculative; experimental studies at the atomic level may prove fruitful. Finally, the low-temperature change in Arrhenius parameters for In remains puzzling; our proposed mechanism involving adatom exchange with steps or kinks would benefit from further evidence.

ACKNOWLEDGMENTS

This work was partially supported by NSF (CTS 98-06329). R.D. and D.L.-R. acknowledge support of DOE (DEFG02-91ER45439) through the Materials Research Laboratory at UIUC.

---

*Author to whom correspondence should be addressed. Electronic address: eseebaue@uiuc.edu

[1] H. Watanabe, A. Sakai, T. Tasumi, and T. Niino, Solid State Technol. **35**, 29 (1992).
[2] M. Inoue, K. Hashizume, and H. Tsuchikawa, J. Vac. Sci. Technol. A **6**, 1636 (1988).
[3] A. G. Naumovets and A. G. Fedorus, Zh. Eksp. Teor. Fiz. **68**, 1183 (1975) [Sov. Phys. JETP **41**, 587 (1976)].
[4] A. G. Fedorus, E. V. Klimenko, A. G. Naumovets, E. M. Zasimovich, and J. N. Zasimovich, Nucl. Instrum. Methods Phys. Res. B **101**, 207 (1995).
[5] K. A. Schultz and E. G. Seebauer, J. Chem. Phys. **97**, 6958 (1992).
[6] C. E. Allen, R. Ditchfield, and E. G. Seebauer, J. Vac. Sci. Technol. A **14**, 22 (1996).
[7] R. Ditchfield, D. Llera-Rodríguez, and E. G. Seebauer, Phys. Rev. Lett. **81**, 1259 (1998).
[8] C. E. Allen, R. Ditchfield, and E. G. Seebauer, Phys. Rev. B **55**, 13 304 (1997).
[9] F. Cerdeira and M. Cardona, Solid State Commun. **7**, 879 (1969).
[10] This mechanism operates only for lightly doped substrates or high illumination intensities, where the photogenerated charge carrier density greatly exceeds the thermal density. See E. G. Seebauer, J. Appl. Phys. **66**, 4963 (1989) for an example.
[11] D. E. Aspnes, Surf. Sci. **37**, 418 (1973).
[12] A. Fujimoto, H. Katsumi, M. Okuyama, and Y. Hamakawa, Jpn. J. Appl. Phys., Part 1 **34**, 804 (1995).
[13] X. Yin, H. M. Chen, F. H. Pollak, Y. Chan, P. A. Montano, P. D. Kirchner, G. D. Pettit, and J. M. Woodall, J. Vac. Sci. Technol. A **10**, 121 (1992).
[14] H. Shen and M. Dutta, J. Appl. Phys. **78**, 2151 (1995).
[15] H. Shen, W. Zhou, J. Pamulapati, and F. Ren, Appl. Phys. Lett. **74**, 1430 (1999).
[16] M. Hecht, Phys. Rev. B **41**, 7918 (1990); J. Vac. Sci. Technol. B **8**, 1018 (1990).
[17] C. R. Carlson, W. F. Buechter, F. Che-Ibrahim, and E. G. Seebauer, J. Chem. Phys. **99**, 7190 (1993).
[18] R. B. Fair, in *Silicon Integrated Circuits* edited by D. Kahng (Academic, New York, 1981), Part B, pp. 1–108.
[19] P. Lautenschlager, M. Garriga, L. Vina, and M. Cardona, Phys. Rev. B **36**, 4821 (1987).
[20] J. Humlicek, F. Lukes, E. Schmidt, M. G. Kekoua, and E. Khoutsishivili, Phys. Rev. B **33**, 1092 (1986).
[21] J. R. Taylor, *An Introduction to Error Analysis: The Study of Uncertainties in Physical Measurements* (University Science Book, Mill Valley, California, 1982).
[22] P. R. Bevington and D. K. Robinson, *Data Reduction and Error Analysis for the Physical Sciences* (McGraw-Hill, New York, 1992).
[23] P. J. Dobsen, *Properties of Silicon* (INSPEC, The Institution of Electrical Engineers, New York, 1988), p. 849.
[24] K. Kondo and A. Moritani, Phys. Rev. B **14**, 1577 (1976).
[25] D. E. Aspnes and J. E. Rowe, Phys. Rev. Lett. **27**, 188 (1971).
[26] H. Shen, S. H. Pan, Z. Hang, J. Leng, F. H. Pollak, J. M. Woodall, and R. N. Sacks, J. Appl. Phys. **53**, 1080 (1988).
[27] T. Kanata, M. Matsunage, H. Takakura, Y. Hamakawa, and T. Nishino, Jpn. J. Appl. Phys., Part 1 **68**, 5309 (1990).
[28] E. H. Rhoderick, *Metal-Semiconductor Contacts* (Clarendon, Oxford, 1978).
[29] A more complete treatment multiplies the right side of Eq. (6) by a term related to surface recombination: $(1+BT^{3/2})^{-1}$. This term becomes significant only above about 600 K for Si, and is therefore neglected here.
[30] J. M. Andrews and M. P. Lepselter, Solid-State Electron. **13**, 1011 (1970).
[31] These additional optical constants include the Seraphin coefficients (Ref. 45) A_2 also contains a factor of T^2, whose contribution to the temperature dependence in the logarithmic terms remains small compared to that embodied by $\exp(V_s/kT)$ and is therefore neglected.
[32] It is well known that the apparent surface potential can change with temperature because of a strong temperature dependence in induced photovoltage (Ref. 44); that is why the method presented gives at best an average value for V_s.
[33] E. G. Seebauer and C. E. Allen, Prog. Surf. Sci. **49**, 265 (1995).
[34] Note that the word ''adatom'' when referring to the details of the Si(111)-(7×7) structure conventionally carries a meaning more specific than the more generic way the term is used throughout this paper.
[35] Y. Wang, X. Chen, and R. J. Hamers, Phys. Rev. B **50**, 4534 (1994); Y. Wang and R. J. Hamers, Phys. Rev. Lett. **74**, 83 (1995).
[36] I. I. Suni and E. G. Seebauer, Surf. Sci. **301**, 235 (1994); Thin Solid Films **272**, 229 (1996).
[37] B. L. Sharma, Defect Diffus. Forum **70&71**, 1 (1990), and references therein.
[38] H. Lim, K. Cho, R. B. Capaz, J. D. Joannopoulos, K. D. Brommer, and B. E. Larson, Phys. Rev. B **53**, 15 421 (1996).
[39] J. J. Lander and J. Morrison, Surf. Sci. **2**, 553 (1964).
[40] M. Horn-von Hoegen, M. Pook, A. Al Falou, B. H. Muller, and M. Henzler, Surf. Sci. **284**, 53 (1993).
[41] F. J. Kimpsel, G. Hollinger, and F. A. Pollak, Phys. Rev. B **28**, 7014 (1983).
[42] F. G. Allen and G. W. Gobeli, Phys. Rev. **127**, 150 (1962); C. Sebenne, D. Bolmont, G. Guichar, and M. Balkanski, Phys. Rev. B **12**, 3280 (1975); W. Eberhart, G. Kalkoffen, C. Kunz, D. Aspnes, and M. Cardona, Phys. Status Solidi B **88**, 135 (1978).

[43] A. Cricenti, D. Purdie, and B. Reihl, Surf. Sci. **331–333**, 1033 (1995).
[44] L. Staufer, S. Van, D. Belmont, J. J. Koulman, and C. Minot, Solid State Commun. **85**, 935 (1993).
[45] J. A. Van Vechten and C. D. Thurmond, Phys. Rev. B **14**, 3539 (1976); **14**, 3551 (1976).
[46] H. Seager and W. K. Schubert, J. Appl. Phys. **62**, 4313 (1987).
[47] C. R. Crowell and S. M. Sze, Solid-State Electron. **9**, 1035 (1966).
[48] A. Many, Y. Goldstein, and N. B. Grover, *Semiconductor Surfaces* (North-Holland, Amsterdam, 1965).
[49] P. T. Landsberg, *Recombination in Semiconductors* (Cambridge University Press, New York, 1991), p. 129.
[50] J. Lagowski, C. L. Balestra, and H. C. Gatos, Surf. Sci. **27**, 547 (1971).
[51] C. E. Allen and E. G. Seebauer, J. Chem. Phys. **104**, 2557 (1996).
[52] D. V. Lang and L. C. Kimerling, Phys. Rev. Lett. **33**, 489 (1974).
[53] J. D. Weeks, J. C. Tully, and L. C. Kimerling, Phys. Rev. B **12**, 3286 (1975).
[54] W. Frank, U. Gosele, H. Mehrer, and A. Seeger, in *Diffusion in Crystalline Solids*, edited by G. E. Murch and A. S. Nowick (Academic, New York, 1984), pp. 64–142.
[55] R. Swalin, J. Appl. Phys. **29**, 670 (1958).
[56] J. R. Hardy and R. Bullough, Philos. Mag. **15**, 237 (1967).
[57] A. D. Brailsford, J. Appl. Phys. **40**, 3087 (1969).
[58] H. Watanabe, A. Sakai, T. Tatsumi, and T. Niino, Solid State Technol. **35**, 29 (1992).
[59] *The National Technology Roadmap for Semiconductors* (Semiconductor Industry Association, San Jose California, 1997).